4

GLYCAN PROFILING OF URINE, AMNIOTIC FLUID AND ASCITIC FLUID FROM GALACTOSIALIDOSIS PATIENTS REVEALS NOVEL OLIGOSACCHARIDES WITH REDUCING END HEXOSE AND ALDOHEXONIC ACID RESIDUES

4.1 ABSTRACT

Urine, amniotic fluid and ascitic fluid samples of galactosialidosis patients were analyzed and structurally characterized for free oligosaccharides using capillary high-performance anion-exchange chromatography with pulsed amperometric detection and online mass spectrometry. In addition to the expected endo-β-*N*-acetylglucosaminidase-cleaved products of complex-type sialylated *N*-glycans, *O*-sulfated oligosaccharide moieties were detected. Moreover, novel carbohydrate moieties with reducing-end hexose residues were detected. On the basis of structural features such as a hexose–*N*-acetylhexosamine–hexose–hexose consensus sequence and di-sialic acid units, these oligosaccharides are thought to represent, at least in part, glycan moieties of glycosphingolipids. In addition, C_1-oxidized, aldohexonic acid containing versions of most of these oligosaccharides were observed. These observations suggest an alternative catabolism of glycosphingolipids in galactosialidosis patients: oligosaccharide moieties from glycosphingolipids would be released by a hitherto unknown ceramide glycanase activity. The results show the potential and versatility of the analytical approach for structural characterization of oligosaccharides in various body fluids.

Cees Bruggink[1,2], Ben J. H. M. Poorthuis[3], Monique Piraud[4], Roseline Froissart[4], André M. Deelder[1] and Manfred Wuhrer[1]

[1] Biomolecular Mass Spectrometry Unit, Department of Parasitology, Leiden University Medical Center, Leiden, The Netherlands
[2] Dionex Benelux BV, Amsterdam, The Netherlands
[3] Department of Medical Biochemistry, Academic Medical Center, Amsterdam, The Netherlands
[4] Laboratoire des Maladies Héréditaires du Métabolisme et Dépistage Néonatal, Centre de Biologie Est, Hospices Civils de Lyon, Bron, France

The FEBS Journal (2010) 277; 2970–2986

4.2 INTRODUCTION

Galactosialidosis is an autosomal recessive lysosomal storage disease, caused by deficiency of both α-neuraminidase (EC 3.2.1.18) and β-galactosidase (EC 3.2.1.23) activities [1], resulting from a defect in the protective protein cathepsin A (EC 3.4.16.5). This lysosomal protein protects α-neuraminidase and β-galactosidase from proteolytic degradation [2] by formation of a complex involving cathepsin A, β-galactosidase, α-neuraminidase and *N*-acetylgalactosamine-6-sulfate sulfatase (EC 3.1.6.4) [3,4].

Galactosialidosis is characterized by excessive excretion of sialyloligosaccharides in the urine, an increase in the amount of bound sialic acid in various tissues, and severe clinical symptoms [5,6]. Three clinical subtypes can be distinguished, depending on the age of onset and severity of the symptoms: the early infantile type with fetal hydrops, ascites, visceromegaly, skeletal dysplasia and early death, usually by 8–12 months of age; the late infantile type with cardiac involvement, hepatosplenomegaly, growth retardation and mild mental retardation; and the juvenile/adult type with progressive neurological deterioration without visceromegaly. Coarse faces, cherry red spots in the macula and vertebral changes are usually present [7,8]. Biochemical diagnosis is made by demonstration of increased excretion of oligosaccharides by thin layer chromatography [9] and by demonstrating a combined deficiency of α-neuraminidase and β-galactosidase in patient cells.

Several activity studies on the structural analysis of sialyloligosaccharides from urine of galactosialidosis patients [10,11] have been published. van Pelt *et al*. [12] described 21 sialylated oligosaccharides. Twenty of these were endo-β-*N*-acetylglucosaminidase-cleaved products of complex-type sialylated *N*-glycans, and one was a di-sialylated diantennary structure with an intact *N,N'*-diacetylchitobiose unit at the reducing end.

Here we report the analysis of oligosaccharides from galactosialidosis patients using a previously described capillary high-performance anion-exchange chromatography (HPAEC) method with combined integrated pulsed amperometric (PAD) and ion-trap mass spectrometric detection and analysis [13]. In addition to urine samples, ascitic fluid and amniotic fluid obtained from mothers pregnant with a galactosialidosis fetus were analyzed. Amniotic fluid is of importance for prenatal diagnosis of many lysosomal storage disorders such as galactosialidosis [14].

In addition to the expected endo-β-*N*-acetylglucosaminidase-cleaved products of complex-type sialylated *N*-glycans, oligosaccharide structures that had not been previously found were detected in the samples from galactosialidosis patients. These newly found oligosaccharide structures included *O*-sulfated oligosaccharide moieties, carbohydrate moieties of glycosphingolipids, and C_1-oxidized (aldohexonic acid) carbohydrate moieties of glycosphingolipids. On the basis of the presence of carbohydrate moieties of glycosphingolipids, we speculate about the potential involvement of a ceramide glycanase in the catabolism of glycosphingolipids in humans.

4.3 RESULTS

Glycans from seven urine samples from six galactosialidosis patients, five amniotic fluid samples from five mothers carrying a fetus suffering from galactosialidosis, and two ascitic fluid samples were analyzed by HPAEC-PAD-MS (Table 4-1). In addition, four urine samples from healthy

Table 4-1. Information about the samples and patients. ND, not detected.

Sample Code	Details	Creatinine (mmol/L)
U1	Urine patient AB, 12 days old, Lyon France	1,0
U2	Urine patient AV, 6 days old, Lyon France	2,3
U3, U4	Urine patient MO, Lyon France	n.d.
U5	Urine patient BO, 127 days old, Lyon France	1,2
U6	Urine patient B07/0175, Amsterdam Netherlands	1,6
U7	Urine patient B07/0845.1, Leiden Netherlands 8 weaks old	0,5
Amfl1	Amniotic fluid patient AB, 30 weeks fetus, Lyon France	n.d.
Amfl2	Amniotic fluid patient AS, 29 weeks fetus, Lyon France	n.d.
Amfl3	Amniotic fluid patient W, 23 weeks of amenorrhoea, Lyon France	n.d.
Amfl4	Amniotic fluid patient LA, 22 weeks fetus, Lyon France	n.d.
Amfl5	Amniotic fluid patient GG, protein 3.5 g/L, Nijmegen Netherlands	0,08
Asf1	Ascite fluid patient AB, Lyon France	n.d.
Asf2	Ascite fluid patient AS, Lyon France	n.d.

individuals were investigated. Figure 4-1 shows a typical HPAEC-PAD chromatogram from a urine sample of a galactosialidosis patient.

4.3.1 *N*-glycan-derived structures

The typical endo-β-*N*-acetylglucosaminidase cleavage products of complex-type *N*-sialyloligosaccharides were found in all urine samples, amniotic fluid samples and ascitic fluid samples (see Fig. 4-2, n1–n6) [12]. A varying number of isomers were detected for the various *N*-glycan compositions, and these were analyzed by MS/MS, as summarized in Table 4-2. *N*-glycan-derived structure n1 had the composition HNS (H, hexose; N, *N*-acetylhexosamine; S, *N*-acetylneuraminic acid), and two isomers of n1 were detected. Tandem mass spectrometry indicated the structure Neu5Ac(α2–3/6)Gal(β1–4)GlcNAc. On the basis of chromatographic retention [15] in combination with the tandem mass spectrometric data [16], we speculate that *N*-acetylneuraminic acid (Neu5Ac) is (α2–6)-linked in the first n1 isomer and (α2–3)-linked in the second isomer. Specifically, the relatively low signal intensity of the fragment ion at *m/z* 655.2 from the second eluting isomer [16] suggests an α2–3-linked Neu5Ac.

Moreover, larger complex sialyloligosaccharides were found with the composition $H_{3-6}N_{2-4}S_{1-3}$. In accordance with literature data [12], we interpreted the three isomers H_3N_2S as sialyl-mono antennary endo-β-*N*-acetylglucosaminidase cleavage products of complex-type *N*-glycan structures (Fig. 4-2, n2). Similarly, the two isomers H_5N_3S were assigned to sialylated diantennary structures (Fig. 4-2, n3), the two isomers $H_5N_3S_2$ as di-sialylated diantennary structures (Fig. 4-2, n4), the two isomers $H_6N_4S_2$ as di-sialylated triantennary structures (Fig. 4-2, n5), and the three isomers $H_6N_4S_3$ as tri-sialylated triantennary structures (Fig. 4-2, n6). These assignments were corroborated by the MS/MS data (Table 4-2).

In addition to the expected endo-β-*N*-acetylglucosaminidase-cleaved products of complex-type sialylated *N*-glycans, some *O*-sulfated versions were also found in low amounts (see Table 4-3 and Fig. 4-2, s1–s4). The detected carbohydrate HSO_3NS eluted in the time window for

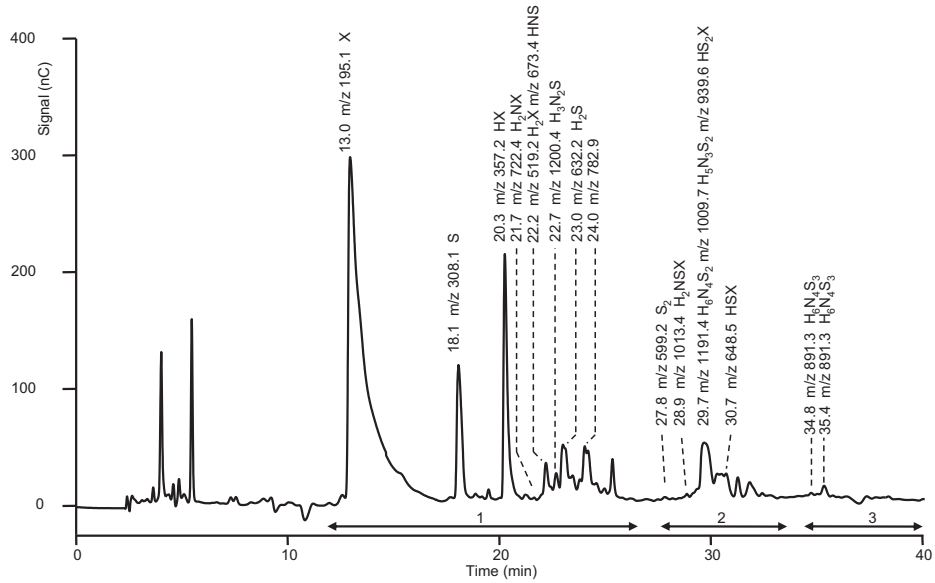

Figure 4-1. Capillary HPAEC-PAD chromatogram of oligosaccharides from a urine sample of a galactosialidosis patient. H, hexose; N, *N*-acetylhexosamine; S, *N*-acetylneuraminic acid; X, aldohexonic acid. The numbers above the horizontal arrows represents the number of acidic groups.

double negatively charged carbohydrates (Fig. 4-1). The MS/MS fragment ions Y_1 (*m/z* 219.9) and Y_2 (*m/z* 462.0) indicated the sequence Neu5Ac–$HexSO_3$–HexNAc (Fig. 4-3). The $^{0,2}A_3$ ring fragment ion at *m/z* 652.1 is typical of a 1–4 glycosidic link [16,17] between $HexSO_3$ and HexNAc.

The lack of significant fragment ions between the fragment ions Y_1 and Y_2 is indicative of a 2–3 linkage between Neu5Ac and $HexSO_3$. These data are consistent with a Neu5Ac(α2–3)Gal-6-SO_3(β1–4) GlcNAc *N*-glycan antenna structure or *O*-glycan structural motif [18]. Moreover, the presence of complex *O*-sulfated sialylated oligosaccharides with the composition $H_{3-5}SO_3N_{2-3}S_{1-2}$ (see Table 4-2), was indicated by MS. Based on observed retention times, mass spectrometric data (Table 4-2) and literature data, these glycans were assigned to sulfated variants of the above-mentioned endo-β-*N*-acetylglucosaminidase cleavage products of complex-type sialylated *N*-glycan structures: the two isomers of composition $H_3SO_3N_2S$ were assigned to *O*-sulfated sialylated monoantennary glycans (Fig. 4-2, s2), the four isomers $H_5SO_3N_3S$ as *O*-sulfated monosialylated diantennary glycans (Fig. 4-2, s3), and the two isomers $H_5SO_3N_3S_2$ as *O*-sulfated, disialylated diantennary glycans (Fig. 4-2, s4).

4.3.2 Glycans with reducing-end hexoses

In addition to the *N*-glycan-derived signals, the LC-MS/MS data provided evidence for the presence of a group of oligosaccharides of composition $H_{0-3}N_{0-1}S_{0-2}$ (g1–g11, Table 4-2). Tandem mass spectrometry indicated a sequence Hex–HexNAc–Hex–Hex or truncated versions thereof for most of these oligosaccharides, decorated with up to two Neu5Ac. Di-sialyl motifs (Neu5Ac linked to Neu5Ac) were also observed. Structural characterization of these oligosaccharides is described below.

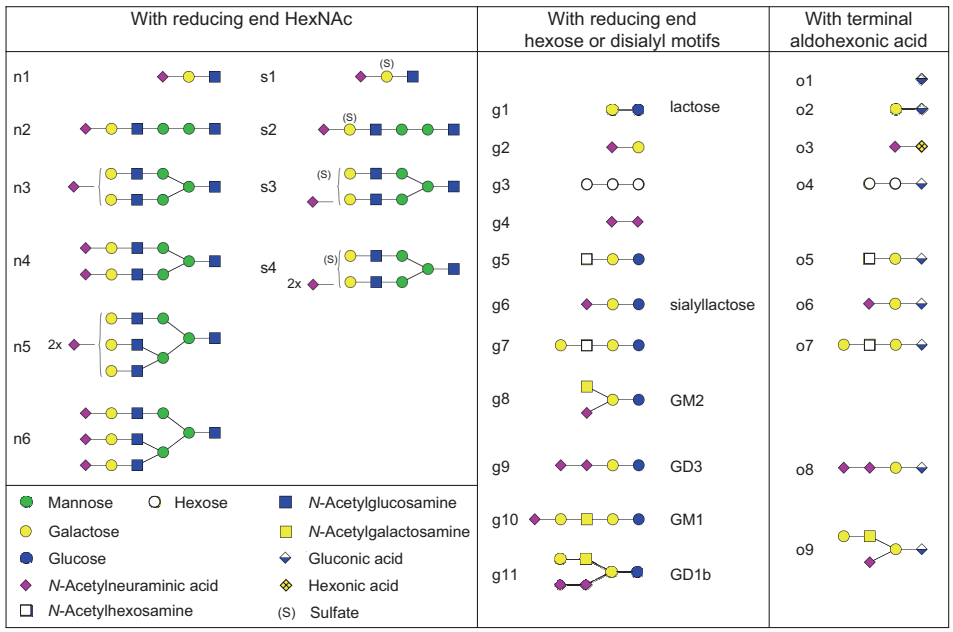

Figure 4-2. Schematic overview of the proposed structures of free oligosaccharides in body liquids from galactosialidosis patients. The codes n1–n6, s1–s4, g1–g11 and o1–o9 refer to Tables 4-2 and 4-3.

Two isomers of the glycan H_2 were detected. The retention time of the late-eluting H_2 isomer was identical to that of maltose (Glc(α1–4)Glc; Table 4-2). The retention time of the early-eluting H_2 isomer was identical to that of lactose, and Fig. 4-4A shows the MS/MS spectrum obtained. Fragment ion C_1 (*m/z* 178.9) indicates the composition H_2 and the ring fragment ion (*m/z* 220.8) corresponds to a loss of 120, which is interpreted as a $^{2,4}A_2$ ring fragment typical of a 1–4 linkage between the hexoses [16,17].

Four isomers were found with the composition H_2S (Table 4-2). The MS/MS spectrum of the first eluting isomer with retention time of 10.5 min is shown in Fig. 4-4B. The fragment ions B_1, C_2, Y_1 and Y_2 indicate the sequence Neu5Ac–Hex–Hex. The ring fragments $^{0,2}A_3$ and $^{0,2}A_3$-18 in combination with lack of the $^{0,3}A_3$ ring fragment ion are typical of a 1–4 linkage between the hexoses [16,17]. The lack of relevant ring fragment ions between fragment ions B_1 and C_2 is indicative of a 2–3 linkage between Neu5Ac and Hex. These combined data are consistent with sialyllactose (Neu5Ac(α2–3)Gal(β1–4)Glc) (g6, Table 4-2). The MS/MS fragmentation spectra of the remaining three isomers with the composition H_2S are indicative of the sequence Neu5Ac–Hex–Hex, for which the structure has been partly elucidated (Table 4-2).

An oligosaccharide species with composition H_2S_2 was detected at 29.1 min (g9, Table 4-2). The fragment ion B_2 (*m/z* 581.2) consists of two *N*-acetylneuraminic acids, indicating a sialic acid–sialic acid motif. Fragment ion Y_3 (*m/z* 632.2) is in accordance with two Hex decorated with Neu5Ac (Fig. 4-4C). These details indicate the sequence Neu5Ac–Neu5Ac–Hex–Hex.

Two isomers were detected with the composition H_3N (*m/z* 706.2) (g7, Table 4-2). The MS/MS spectrum of the isomer eluting at 12.7 min is shown in Fig. 4-4D. The fragment ions B_2 (*m/z*

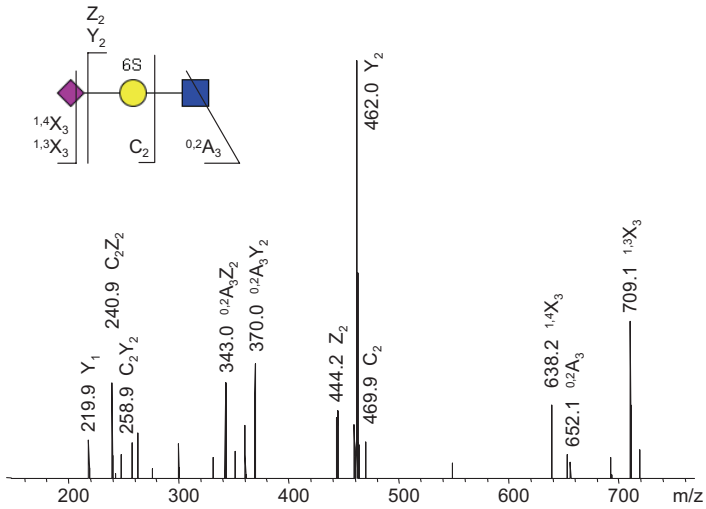

Figure 4-3. Negative-ion fragmentation spectrum of the proposed 6'-sulfated sialyl lactosamine.

363.5) and C_2 (*m/z* 381.9) corresponded to Hex linked to HexNAc. The fragments C_3 (*m/z* 543.9) and C_2 (*m/z* 381.9) indicated two Hex at the reducing end. Based on the ring fragment ions $^{0,2}A_4$ and $^{0,2}A_4$-18 and the lack of $^{0,3}A_4$, a 1–4 linkage was deduced for the two hexoses at the reducing terminus [16,17], in accordance with a lactose core structure. From the combined data, we postulate that this oligosaccharide has the glycan structure Hex–HexNAc–Gal(β1–4)Glc.

Two isomers with the composition H_3NS were detected at *m/z* 997.3 (g10, Table 4-2). The MS/MS spectrum of the isomer eluting at 22.0 min is shown in Fig. 4-4E. The fragment ions B_1, C_1, B_2, C_2, B_3, C_3, and C_4 are indicative of the sequence Neu5Ac–Hex–HexNAc–Hex–Hex. The proposed linear sequence was supported by the abundant signals B_3 and C_3. The lack of ring fragments between C_2 and C_1 is indicative of a 2–3 linkage between Neu5Ac and the adjacent hexose. No relevant ring fragments were observed between C_2 and C_3, which is consistent with a 1–3 linkage between Hex and HexNAc. The ring fragment ions $^{0,2}A_4$ and $^{2,4}A_4$, and the lack of $^{0,3}A_4$, are indicative of a 1–4 linkage between HexNAc and the adjacent hexose. The ring fragment ions $^{0,2}A_5$, $^{0,2}A_5$-18 and $^{2,4}A_5$, and the lack of $^{0,3}A_5$, are indicative of a 1–4 link between the reducing end Hex and the adjacent Hex [16,17]. Based on these data, we propose the structure Neu5Ac(α2–3)Hex(β1–3)HexNAc(β1–4)Gal(β1–4)Glcβ.

An oligosaccharide of composition $H_3N_1S_2$ was detected (g11, Table 4-2). MS/MS analyses revealed an intense signal at *m/z* 563.6 ($B_{2\alpha}$-H_2O), which indicates a di-sialic acid motif. This oligosaccharide was interpreted to be an extended version of g9, and the structure Hex–HexNAc–(Neu5Ac–Neu5Ac)–Hex–Hex is proposed. Moreover, a Neu5Ac–Neu5Ac disaccharide was detected (g4, Table 4-2), as well as oligosaccharides of composition H_2F_1 (where F stands for deoxyhexose) and $H_2N_1F_1$ (Table 4-2).

4.3.3 Glycans with aldohexonic acid

In addition, evidence was obtained from the LC–MS/MS data for the presence of C_1-oxidized glycans (Fig. 4-2, o1–o9). The innermost residue of these oligosaccharides was found to be

Table 4-2. Structural data for detected oligosaccharides moieties.

Glycan composition	Species	Ret. time (min)	Signal m/z	MS/MS fragment ions	Proposed Structures	
HNS	n1	22,3	673.6 [M-H]$^-$	655.2 -H_2O; 572.2 $^{0,2}A_3$; 544.2 $^{0,2}A_3$-H_2O; 512.1 $^{2,4}A_3$; 470.1 C_2; 452.1 B_2; 410.1 $^{0,2}A_2$;392.2 $^{0,2}A_2$-H_2O; 380.2 $^{0,3}A_2$; 350.1 $^{0,4}A_2$; 332.1 $^{0,4}A_2$-H_2O; 308.0 C_1; 290.0 B_1	Fig. 2 n1	Neu5Ac(α2–6)Gal(β1–4)GlcNAc
		26,9	673.6 [M-H]$^-$	655.2 -H_2O; 572.2 $^{0,2}A_3$; 544.2 $^{0,2}A_3$-H_2O; 512.0 $^{2,4}A_3$; 470.1 C_2; 452.2 B_2; 410.2 $^{0,2}A_2$;392.2 $^{0,2}A_2$-H_2O; 380.0 $^{0,3}A_2$; 308.0 C_1; 290.0 B_1	Fig. 2 n1	Neu5Ac(α2–3)Gal(β1–4)GlcNAc
H_3N_2S	n2	22,3	1200.4 [M-H]$^-$	1182.6 -H_2O; 1122.5; 1099.4 $^{0,2}A_6$; 1081.3 $^{0,2}A_6$-H_2O; 998.2; 979.3 B_5; 943.3; 937.3 $^{0,2}A_5$; 835.4 C_4; 818.5; 747.9 $^{2,4}A_5Y_5$; 728.8 Z_4; 686.6 $^{2,4}X_4$; 655.0 B_3; 536.2	Fig. 2 n2	Neu5Ac(α2–3/6)Gal(β1–4) GlcNAc(β1–2)Man(α1–6)Man(β1–4) GlcNAc
		22,5	1200.4 [M-H]$^-$; 1298.5 [M+H_2SO_4-H]$^-$	1182.6 -H_2O; 1122.5; 1099.5 $^{0,2}A_6$; 1081.5 $^{0,2}A_6$-H_2O; 1039.5 $^{2,4}A_6$; 997.5 C_5; 979.6 B_5; 835.4 C_4; 817.4 B_4; 748.4 $^{2,4}A_5Y_5$; 673.4 C_3; 655.4 B_3; 572.3 $^{0,2}A_3$; 526.1 $^{3,5}A_3$; 470.2 C_2; 452.2 B_2; 424.2 $^{1,5}A_2$; 410.1 $^{0,2}A_3$	Fig. 2 n2	Neu5Ac(α2–6)Gal(β1–4)GlcNAc(β1–2)Man(α1–3)Man(β1–4)GlcNAc
		23,3	1200.4 [M-H]$^-$; 1298.5 [M+H_2SO_4-H]$^-$	1182.4 -H_2O; 1165.1; 1122.5; 1099.4 $^{0,2}A_6$; 1081.3 $^{0,2}A_6$-H_2O; 1063.4; 1039.3 $^{2,4}A_6$; 1021.4; 997.3 C_5; 979.2 B_5; 961.2; 910.4; 835.2 C_4; 819.2 $^{0,3}X_5$; 817.2 B_4; 784.4; 779.4; 791.1; 775.4 $^{0,2}A_4$; 773.4; 748.2 $^{2,4}A_5Y_5$; 744.3; 696.3; 674.0; 672.4; 655.3 B_3; 619.1; 592.3; 586.1; 568.0; 554.2 $^{0,2}A_3$-H_2O; 536.1; 526.1 $^{3,5}A_3$; 424.1 $^{1,5}A_2$; 381.1	Fig. 2 n2	Neu5Ac(α2–3)Gal(β1–4)GlcNAc(β1–2) Man(α1–3)Man(β1–4)GlcNAc
H_5N_3S	n3	23,7	1727.8 [M-H]$^-$	1709.8 -H_2O; 1668.8 $^{2,4}X_5$; 1626.7 $^{0,2}A_6$; 1608.7 $^{0,2}A_6$-H_2O; 1566.7 $^{2,4}A_6$; 1524.7 C_5; 1506.8 B_5; 1316.6 $^{0,2}X_{5\beta}Y_{5\alpha}$; 1275.5 $^{2,4}A_6Y_{5\alpha}$; 1113.6 $^{2,4}A_6Y_{4\alpha}$; 1053.7 $Z_{3\alpha}$; 979.3 $C_{5\alpha}Z_{2\beta}$; 961.3 $B_{5\alpha}Z_{2\beta}$; 835.3 $C_{4\alpha}$; 817.4 $B_{4\alpha}$	Fig. 2 n3	Neu5Ac(α2–3/6)Gal(β1–4) GlcNAc(β1–2)Man(α1–6)(Gal(β1–4) GlcNAc(β1–2)Man(α1–3))Man(β1–4) GlcNAc
		27,6	1727.8 [M-H]$^-$		Fig. 2 n3	
$H_5N_3S_2$	n4	27,3	1009.0 [M-2H]$^{2-}$	1709.6 $Z_{5\alpha\beta}$; 1626.6 $^{0,2}A_6Y_{5\alpha}$; 1548.7 $^{2,4}A_6Z_{5\alpha}$; $C_5Y_{5\alpha}$; 1050.5; 1000.3 -H_2O; 958.9 $^{0,2}A_6$; 907.8 $^{0,3}A_{5\beta}$; 835.6 C_4; 817.7 B_4; 655.6 B_3; 290.2 B_1	Fig. 2 n4	Neu5Ac(α2–6)Gal(β1–4)GlcNAc(β1–2)Man(α1–6)(Neu5Ac(α2–6) Gal(β1–4)GlcNAc(β1–2)Man(α1–3)) Man(β1–4)GlcNAc
		28	1009.0 [M-2H]$^{2-}$	1797.6 B_5; 1727.6 Y_5; 1709.6 Z_5; 1626.6 $^{0,2}A_6Y_5$; 1608.5 $^{0,2}A_6Z_5$; 1566.4 $^{2,4}A_6Y_5$; 1524.5 C_5Y_5; 1000.4 -H_2O; 958.8 $^{0,2}A_6$; 907.4 $^{0,3}A_{5\beta}$; 835.3 C_4; 817.3 B_4; 673.2 C_3; 655.3 B_3; 452.1 B_2; 424.1 $^{1,5}A_2$; 410.1 $^{0,2}A_2$; 350.0 $^{0,4}A_2$; 307.9 C_1; 290.0 B_1	Fig. 2 n4	Neu5Ac(α2–3/6)Gal(β1–4) GlcNAc(β1–2)Man(α1–6) (Neu5Ac(α2–3/6)Gal(β1–4) GlcNAc(β1–2)Man(α1–3))Man(β1–4) GlcNAc

$H_6N_4S_2$	n5	27,4	1191.4 $[M-2H]^{2-}$		Fig. 2 n5	
		31,4	1191.4 $[M-2H]^{2-}$		Fig. 2 n5	
$H_6N_4S_3$	n6	31,3	891.3 $[M-2H]^{3-}$; 1337.4 $[M-2H]^{2-}$	2075.8; 2074.9 Z_6Y_6 or Y_6Z_6; 2016.0; 1995.1; 1992.9; 1974.6; 1973.8; 1931.8; 1890.6; 1889.8; 1871.8; 1608.4; 1474.4; 1473.6 $B_{4\alpha}$; 1328.7 $-H_2O$; 1279.1 $^{1,4}X_{6\alpha,\beta,\gamma}$; 1203,4; 1202.3; 1201.3; 1200.5 $C_{4\alpha}Y_{5\alpha}$; 1192.1; 1191.4 Y_5; 1184.7; 1183.9; 1182.4 Z_5; 1152.8; 1142.7; 1141.0; 1133.6; 1132.8; 1111.5; 1111.1; 1092.6; 1090.0 $C_5Y_{5\alpha}$; 1081.4; 1039.7; 1009.3; 1000.3; 981.0; 979.2 $B_5Y_{2\alpha}$; 963.3; 962.2 $B_5Z_{2\alpha}$; 944.4; 907.2 $C_5Y_{3\alpha}$; 885.5 $-H_2O$; 879.0; 860.0; 857.3 $^{0,2}A_6$; 852.0 $^{2,5}X_6$; 851.1 $^{0,4}X_6$; 838.1; 837.4 $^{2,4}A_6$; 835.5 C_4; 823.3 C_5; 817.2 B_4; 798.3; 775.2 $^{0,2}A_4$; 750.0; 745.3 $C_{4\alpha}$; 737.2; 736.1; 673.3 C_3; 655.2 B_3; 536.1; 470.1 C_2; 424.1 $^{1,5}A_2$; 306.2; 290.0 B_1;	Fig. 2 n6	Neu5Ac(α2–3)Gal(β1–4)GlcNAc(β1–2)Man(α1–6)(Neu5Ac(α2–3)Gal(β1–4)GlcNAc(β1–2)(Neu5Ac(α2–6)Gal(β1–4)GlcNAc(β1–4))Man(α1–3))Man(β1–4)GlcNAc
		32,4	891.3 $[M-2H]^{3-}$		Fig. 2 n6	
		34,6	891.3 $[M-2H]^{3-}$		Fig. 2 n6	
HSO_3NS	s1	32	753.2 $[M-H]^-$; 851.1 $[M+H_2SO_4-H]^-$	709.1 $^{1,3}X_3$; 652.1 $^{0,2}A_3$; 638.2 $^{1,4}X_3$; 469.9 C_2; 462.0 Y_2; 444.2 Z_2; 370.0; 361.1 $^{0,2}A_3Y_2$; 352.0; 343.0 $^{0,2}A_3Z_2$; 331.9 $B_2^{0,4}X_3$-SO_3; 301.0 $^{2,4}A_3Y_2$; 276.8 $B_2^{3,5}X_3$-SO_3; 263.8 $^{0,2}A_3Z_2$-SO_3; 258.9 C_2Y_2; 248.9 $C_2^{0,2}X_3$-SO_3; 240.9 C_2Z_2; 219.9 Y_1	Fig. 2 s1	NeuAc(α2-3)Gal(6S)(β1-4)GlcNAc
$H_3SO_3N_2S$	s2	36,5	639.7 $[M-2H]^{2-}$	990.2; 989.2 Y_5; 987.0 $^{0,3}A_5$; 971.1 $^{3,5}A_5$; 951.2 $^{1,5}A_5$-SO_3; 915.3 C_4; 890.2; 888.2 $^{0,2}A_6Y_5$; 886.1 $C_5^{0,3}X_6$; 871.5 $C_4^{1,3}X_6$; 870.1 $^{0,2}A_6Z_5$; 829.5; 828.2 $^{2,4}A_6Y_5$; 786.1 C_5Y_5; 768.0 C_5Z_5; 726.2 $C_5^{1,3}X_5$; 693.9 $C_4^{0,2}X_6$; 655.1 B_3-SO_3; 647.8 $^{2,4}A_5Z_5$; 630.6 $-H_2O$; 629.5 $C_3^{1,3}X_6$-SO_3; 624.1 C_4Y_5; 622.2 $^{0,3}A_3$; 620.3 $B_2^{1,4}X_6$; 611.3 $B_3^{1,3}X_6$-SO_3; 600.5 $^{3,5}A_6Y_4$; 594.1; 589.1 $^{0,2}A_6$; 588.1 B_4Z_5; 580.1; 571.9 $C_5^{1,5}X_5$; 559.0 $^{2,4}A_6$; 541.1 $^{2,5}A_6$-SO_3; 538.6; 58.1 C_5; 537.0 $^{2,5}X_6$; 529.1 B_5; 519.1 $^{2,4}X_6$-SO_3; 516.1 $C_5^{1,3}X_6$; 484.0 $C_5^{2,4}X_4$; 478.5 $^{0,4}A_3$; 470.0 C_2; 457.0 C_4; 449.0 $C_2^{2,4}X_6$; 448.1 B_4; 444.0 C_3Z_5; 427.5 $C_5^{0,2}X_6$; 418.8 $B_5^{0,2}X_6$; 398.0 $^{1,5}A_3Z_5$; 397.6 $B_4^{2,4}X_6$; 397.0 $^{3,5}A_6Y_3$; 380.0 $^{1,4}A_2$; 375.9 C_3; 357.1 $B_2^{3,5}X_6$; 302.1 $^{3,5}A_3$; 292.7 $^{2,4}A_6Y_5$; 290.0 B_1; 215.3 $B_2^{2,4}X_6$; 210.8 $B_4^{2,5}X_4$	Fig. 2 s2	Neu5Ac(α2–3)Gal(6S)(β1–4)GlcNAc(β1–2)Man(α1–6)Man(β1–4)GlcNAc
		38,9	639.7 $[M-2H]^{2-}$		Fig. 2 s2	Neu5Ac(α2–3/6)Gal(6S)(β1–4)GlcNAc(β1–2)Man(α1–3)Man(β1–4)GlcNAc

Table 4-2. continued.

Glycan composition	Species	Ret. time (min)	Signal m/z	MS/MS fragment ions	Proposed Structures	
$H_5SO_3N_3S$	s3	34,6	903.3 $[M\text{-}2H]^{2-}$	1446.3 $^{0,2}A_5Z_{4\beta}$; 886.4; 859.2; 826 $^{3,5}X_{5\beta}$; 774.1 $^{2,5}A_6Z_{2\alpha}$; 757.6 E_3-ion; 638.1 $B_5Z_{5\alpha}$; 613.2 $^{2,5}A_6Z_{3\beta}$; 612.2 $B_{4\alpha}$ $^{2,5}X_{6\alpha}$; 595.0; 594.2 $^{3,5}A_6Z_{4\alpha}$; 483.1 $Y_{3\alpha}$ $^{2,5}X_{5\beta}$; 308.1 C_1; 290.3 B_1	Fig. 2 s3	Gal(6S)(β1–4)GlcNAc(β1–2) Man(α1–6)(Neu5Ac(α2–3)Gal(β1–4) GlcNAc(β1–2)Man(α1–3))Man(β1–4) GlcNAc
		39,3	903.3 $[M\text{-}2H]^{2-}$		Fig. 2 s3	
		41,4	903.3 $[M\text{-}2H]^{2-}$		Fig. 2 s3	
		45,4	903.3 $[M\text{-}2H]^{2-}$		Fig. 2 s3	
$H_5SO_3N_3S_2$	s4	39,6	1048.8 $[M\text{-}2H]^{2-}$		Fig. 2 s4	Neu5Ac(α2–3/6)Gal(6S)(β1–4) GlcNAc(β1–2)Man(α1–6) (Neu5Ac(α2–3/6)Gal(β1–4) GlcNAc(β1–2)Man(α1–3))Man(β1–4) GlcNAc
H_2	g1	7,6	341.2 $[M\text{-}H]^-$	323.0 $-H_2O$; 220.8 $^{2,4}A_2$; 178.9 C_1	Fig. 2 g1; Fig. 4A	Gal(β1–4)Glc
		8,2	341.2 $[M\text{-}H]^-$; 439.1 $[M+H_2SO_4\text{-}H]^-$	281.0 $^{0,2}A_2$; 235.0 $^{3,5}A_2$; 220.8 $^{2,4}A_2$; 178.9 C_1; 160.9 B_1		Glc(α1–4)Glc
HS	g2	24,4	470.2 $[M\text{-}H]^-$	410.0 $^{0,2}A_2$; 379.9 $^{0,3}A_2$; 370.0; 308.0 C_1; 290.0 B_1; 271.8; 220.0; 194.8; 169.9		NeuAc(α2–6)Gal
		25,1	470.2 $[M\text{-}H]^-$; 568.2 $[M+H_2SO_4\text{-}H]^-$	357.8; 307.8 C_1; 290.0 B_1; 272.9; 269.7; 219.8; 201.7; 173.8; 169.9	Fig. 2 g2	NeuAc(α2–3)Gal
H_3	g3	7,6	503.2 $[M\text{-}H]^-$; 601.2 $[M+H_2SO_4\text{-}H]^-$	369.2 $^{1,5}X_3$; 341.1 C_2; 323.1 B_2; 281.0 $^{0,2}A_2$; 262.8 $^{0,2}A_2\text{-}H_2O$; 234.8 $^{3,5}A_2$; 221.0 $^{2,4}A_2$; 202.9 $^{2,4}A_2\text{-}H_2O$; 178.9 C_1; 160.9 B_1		Hex(1–4)Hex(1–3)Hex
		9,1	503.2 $[M\text{-}H]^-$; 601.2 $[M+H_2SO_4\text{-}H]^-$	341.1 C_2; 323.1 B_1; 250.9 $^{0,3}A_2$; 220.9 $^{0,4}A_2$; 178.9 C_1; 160.9 B_1		Hex(1–6)Hex(1–3)Hex
		20,4	503.2 $[M\text{-}H]^-$; 601.2 $[M+H_2SO_4\text{-}H]^-$	443.4 $^{0,2}A_3$; 424.7 $^{0,2}A_3\text{-}H_2O$; 383.1 $^{2,4}A_3$; 341.1 C_2;322.8 B_2; 295.4 $^{1,5}A_2$; 280.9 $^{0,2}A_2$; 237.0 $^{2,5}X_2$; 234.7 $^{3,5}A_2$; 220.8 $^{2,4}A_2$; 178.9 C_1; 160.8 B_1	Fig. 2 g3	Gal(α1–4)Gal(β1–4)Glc
S_2	g4	27,7	599.2 $[M\text{-}H]^-$; 697.2 $[M+H_2SO_4\text{-}H]^-$	581.1 $-H_2O$; 511.1 $^{0,2}A_2$; 495.0 $^{2,5}A_2$; 410.0 $^{0,4}A_2$; 380.0 $^{1,5}X_2$; 308.0 C_1; 290.0 B_1		Neu5Ac(α2–8)Neu5Ac
		25,5	599.2 $[M\text{-}H]^-$			

H_2N	g5	9,6	544.2 $[M-H]^-$; 642.2 $[M+H_2SO_4-H]^-$	526.1; 383.0; 290.0; 271.9; 169.9	Fig. 2 g5	GlcNAc(β1–4)Gal(β(–4)Glc
H_2S	g6	10,5	632.2 $[M-H]^-$; 730.2 $[M+H_2SO_4-H]^-$	614.0 -H_2O; 588.1 $^{1,3}X_3$; 572.1 $^{0,2}A_3$; 554.0 $^{0,2}A_3$-H_2O; 535.9; 470.0 C_2; 411.0 $^{0,2}X_3$; 408.0; 385.9; 341.1 Y_2; 290.0 B_1; 178.9 Y_1	Fig. 2 g6; Fig. 4B	Neu5Ac(α2–3)Gal(β1–4)Glc
		13,3	632.2 $[M-H]^-$; 730.2 $[M+H_2SO_4-H]^-$	614.0 -H_2O; 598.6; 588.1 $^{1,3}X_3$; 534.3; 532.3; 472.1; 470.9; 469.9 C_2; 456.2; 411.0 $^{0,2}X_3$; 341.1 Y_2; 307.9 C_1; 290.0 B_1; 178.9 Y_1		Neu5Ac(α2–3)Hex(1–3)Hex or Neu5Ac(α2–3)Gal(1–3)Gal
		14,6	632.2 $[M-H]^-$; 730.2 $[M+H_2SO_4-H]^-$	614.0 -H_2O; 599.1; 588.1 $^{1,3}X_3$; 535.0; 534.2; 524.1; 472.2; 470.1 C_2; 411.1 $^{0,2}X_3$; 434.0; 416.1; 411.0; 408.0 B_2 $^{1,3}X_3$; 404.0; 386.0; 341.0 Y_2; 337.0 B_2 $^{1,4}X_3$; 305.9 $^{0,4}A_2$-CO_2; 292.0; 290.0 B_1; 178.8 Y_1		Neu5Ac(α2–6)Hex(1–3)Hex or Neu5Ac(α2–6)Gal(β1–3)Glc
		20,9	632.2 $[M-H]^-$; 730.2 $[M+H_2SO_4-H]^-$	614.0 -H_2O; 572.1 $^{0,2}A_3$; 571.2; 554.1 $^{0,2}A_3$-H_2O; 536.0; 512.1 $^{2,4}A_3$; 494.0 $^{2,4}A_3$-H_2O; 472.0; 470.1 C_2; 468.1; 452.0 B_2; 441.0 $^{0,3}X_3$; 411.0 $^{0,2}X_3$; 410.0 $^{0,2}A_2$; 408.1; 392.1 $^{0,2}A_2$-H_2O; 380.0 $^{0,3}A_2$; 350.0 $^{0,4}A_2$; 334.0; 332.0; 316.0; 308.0 C_1; 306.0 $^{0,4}A_2$-CO_2; 290.0 B_1		Neu5Ac(α2–6)Hex(1-4)Glc or Neu5Ac(α2–6)Gal(β1–4)Glc
H_3N	g7	9,5	706.2 $[M-H]^-$; 804.3 $[M+H_2SO_4-H]^-$	688.0 -H_2O or D-ion; 646.2 $^{0,2}A_4$; 628.1 $^{0,2}A_4$-H_2O; 585.6 $^{0,4}A_4$; 544.1 C_3; 424.2 $^{1,3}A_3$; 382.0 C_2; 280.9 $^{0,2}A_2$; 263.0 $^{0,2}A_4Z_2$		Gal(β1–4)GlcNAc(β1–2)Man(α1–6) Man
		12,7	706.2 $[M-H]^-$; 804.3 $[M+H_2SO_4-H]^-$; 902.3 $[M+2H_2SO_4-H]^-$	646.3 $^{0,2}A_4$; 628.1 $^{0,2}A_4$-H_2O; 543.9 C_3;381.9 C_2;363.5 B_2;202.1 C_2Z_3	Fig. 2 g7; Fig. 4D	Gal(β1–3)GalNAc(β1–4)Gal(β1–4)Glc
H_2NS	g8	22,8	835.3 $[M-H]^-$	817.3 -H_2O; 715.2 $^{2,4}A_3$; 673.0 C_3; 655.3 B_3; 572.0 $^{0,2}A_3Y_{2\beta}$; 494.2 $^{2,4}A_3Z_{2\beta}$; 290.1 $B_{1\alpha}$	Fig. 2 g8	GalNAc(β1–4)[Neu5Ac(α2–3)] Gal(β1–4)Glc
H_2S_2	g9	29,1	923.3 $[M-H]^-$	632.2 Y_3; 581.1 B_2; 538.1 B_3 $^{2,5}X_4$; 379.9 C_2 $^{1,5}X_4$; 290.0 B_1; 178.9 Y_1	Fig. 2 g9; Fig. 4C	Neu5Ac(α2–8)Neu5Ac(α2–3) Gal(β1–4)Glc
H_3NS	g10	22	997.3 $[M-H]^-$; 1095.3 $[M+H_2SO_4-H]^-$	979.2 –H_2O; 937.2 $^{0,2}A_5$; 920.1; 919.2 $^{0,2}A_5$-H_2O; 877.0 $^{2,4}A_5$; 835.1 C_4; 818.4; 776.5 $^{0,2}A_4$; 717.1; 715.1 $^{2,4}A_4$; 673.2 C_3; 655.3 B_3; 595.1; 586.1; 572.0 $^{1,5}X_4$; 555.4; 554.3 B_3 $^{2,4}X_5$; 526.2 Z_3; 511.9 $^{2,4}A_3$; 470.1 C_2; 452.2 B_2; 379.8; 383.0; 351.0 B_2 $^{2,4}X_3$; 332.0 B_2 $^{0,4}X_5$; 308.0 C_1; 290.0 B_1	Fig. 2 g10; Fig.4E	Neu5Ac(α2–3)Gal(β1–3)GalNAc(β1–4) Gal(β1–4)Glc
		24	997.3 $[M-H]^-$; 1095.3 $[M+H_2SO_4-H]^-$			
H_3NS_2	g11	29,5	643.7 $[M-2H]^{2-}$	999.4; 998.2; 997.4 $Y_{3\alpha}$; 563.6 $B_{2\alpha}$-H_2O; 562.6 C_3; 471.1; 290.0 $B_{1\alpha}$; 271.9 $B_{1\alpha}$-H_2O	Fig. 2 g11	Gal(β1–3)GalNAc(β1–4)[Neu5Ac(α2–8)Neu5Ac(α2–3)]Gal(β1–4)Glc
X	o1	13,3	195.1 $[M-H]^-$		Fig. 2 o1	GluconA
HX	o2	19,2	357.2 $[M-H]^-$; 455.1 $[M+H_2SO_4-H]^-$	339.1 -H_2O; 321.0; 297.1 $^{2,4}X_2$; 277.2; 258.7; 237.0 $^{0,2}X_2$; 220.9 $^{2,4}A_2$; 195.0 Y_1; 178.9 C_1; 176.9 Z_1; 160.9 B_1; 158.9 Z_1-H_2O	Fig. 2 o2; Fig. 5A	Gal(β1–4)GluconA
SX	o3	26,4	486.1 $[M-H]^-$		Fig. 2 o3	

Table 4-2. continued.

Glycan composition	Species	Ret. time (min)	Signal m/z	MS/MS fragment ions	Proposed Structures	
H_2X	o4	22,6	519.2 $[M-H]^-$; 617.1 $[M+H_2SO_4-H]^-$	382.7 $^{2,4}A_3$; 356.9 Y_2; 297.5 $^{2,4}X_2$ or $^{0,2}A_3Y_2$; 221.0 $^{2,4}A_2$; 177.1 Z_1; 161.0 B_1	Fig. 2 o4	Gal(α1–4)Gal(β1–4)GluconA
HNX	o5	24,3	560.2 $[M-H]^-$; 658.2 $[M+H_2SO_4-H]^-$	406.8; 399.0; 398.1; 396.0; 394.8; 323.0; 235.8; 179.0; 160.9	Fig. 2 o5	
		38,2	560.2 $[M-H]^-$	543.0; 540.9; 516.0; 480.0; 463.0; 462.2; 445.1; 349.2; 348.1; 345.0; 284.8	Fig. 2 o5	
HSX	o6	26	648.5 $[M-H]^-$	630.2 $-H_2O$; 604.3 $-CO_2$; 586.6 $-H_2CO_3$; 544,2 $-C_3H_4O_4$; 510.2; 491.2; 428.0; 357.1 Y_2; 339.0 Z_2; 310.7 $^{1,5}A_3Y_2$; 307.9 C_1	Fig. 2 o6; Fig. 5B	Neu5Ac(α2–3)Gal(β1–4)GluconA
H_2NX	o7	21,4	722.4 $[M-H]^-$; 820.3 $[M+H_2SO_4-H]^-$	704.2 $-H_2O$; 628.2; 602.3 $^{0,2}X_4$; 586.2 $[M-CH_2OH(CHOH)_2CO_2H-H]^-$; 560.2 Y_3; 543.9 C_3; 421.8; 406.1 Z_3-$(CH_2OH(CHOH)_2CO_2H)$; 402.7; 357.0 Y_2; 298.2; 267.9; 262.7; 234.0; 220.9 C_2Y_3	Fig. 2 o7; Fig. 5D	Gal(β1–3)GalNAc(β1–4)Gal(β1–4) GluconA
HS_2X	o8	29,4	939.6 $[M-H]^-$	895.4 $-CO_2$; 841.5; 648.3 Y_3; 604.2 Y_3-CO_2; 581.3 B_2; 370.0; 357.1 Y_2; 290.0 B_1	Fig. 2 o8; Fig. 5C	Neu5Ac(α2–8)Neu5Ac(α2–3) Gal(β1–4)GluconA
H_2NSX	o9	27,4	1013.4 $[M-H]^-$; 1111.4 $[M+H_2SO_4-H]^-$	995.5 $-H_2O$; 969.7 $-CO_2$; 951.7 $-H_2CO_3$; 909.5 $-C_3H_4O_4$; 817.5 B_3; 722.3 $Y_{2\beta}$; 704.1 $Z_{2\beta}$; 537,2; 406.2 $Z_{3\alpha}Z_{2\beta}$-$(CH_2OH(CHOH)_2CO_2H$; 380.1; 364.1 $B_{2\alpha}$; 357.1 $Y_2Y_{2\beta}$	Fig. 2 o9; Fig. 5E	Gal(β1–3)GalNAc(β1–4)[Neu5Ac(α2–3)]Gal(β1–4)GluconA
		30,8	1013.4 $[M-H]^-$			
H_2F		8,5	487.2 $[M-H]^-$; 585.3 $[M+H_2SO_4-H]^-$	426.9 $^{0,2}A_3$; 409.0 $^{0,2}A_3-H_2O$; 325.1 C_2; 306.9 B_2; 295.0 $^{1,5}A_3Y_2$; 246.0 $^{2,5}A_3Z_2$; 204.9 $^{1,3}A_2$; 178.9 Y_1; 162.9 C_1; 160.9 Z_1		Fuc(α1–2)Gal(β1–4)Glc
H_2NF		7	690.2 $[M-H]^-$; 788.3 $[M+H_2SO_4-H]^-$	592.1; 528.0 $C_{2\alpha}$; 526.7; 363.9 $C_{2\alpha}Z_{2\beta}$; 348.1 $C_{2\alpha}Z_{2\alpha}$; 347.7; 244.0 $^{2,4}A_{2\alpha}$/ $Z_{2\alpha}Y_{2\beta}$; 212.0		Hex(1–3)(Fuc4/3)HexNAc(1–4)Hex

an aldohexonic acid (X) with a carboxyl group at C_1. This monosaccharide differs by +16 Da from hexose and by +2 Da from hexuronic acid (oxidation of the alcohol group at C_6). The aldohexonic acid-containing oligosaccharides (o1–o9) showed close structural similarities to the above-mentioned glycans with reducing-end hexose oligosaccharides (g1–g11). The structural interpretation obtained for these glycans is presented below.

A component at *m/z* 357.2 was detected and interpreted as HX on the basis of the MS/MS spectrum (Fig. 4-5A). Fragment ion B_1 (*m/z* 160.9) and C_1 (*m/z* 178.9) indicate terminal hexose, and Z_1 (*m/z* 176.9) and Y_1 (*m/z* 195.0) result from aldohexonic acid. The fragment ion with mass *m/z* 158.9 is interpreted as a mass loss of 18 Da from the Z_1 ion. For the fragment ion with mass *m/z* 220.9, carbon chain cleavages at C_2–C_3 and C_4–C_5 of the aldohexonic acid were assumed. A linkage of hexose to the C_4 of aldohexonic acid is postulated. The proposed structure for HX is Gal(β1–4)GluconA (gluconic acid), which may be interpreted as the C_1-oxidized form of lactose.

A glycan with the composition HSX (*m/z* 648.5) was detected at retention time 26.0 min (Table 4-2). The MS/MS spectrum is shown in Fig. 4-5B. The fragment ions C_1 (*m/z* 307.9), Y_2 (*m/z* 357.1), Z_2 (*m/z* 339.0) and $[M–CH_2OCH_2OCOO–H]^-$ (*m/z* 544.2) are indicative of the sequence Neu5Ac–Hex–HexonA (aldohexonic acid). Fragment ions at *m/z* 604.3 $[M–CO_2–H]^-$ and (*m/z* 586.3) $[M–CO_2–H_2O–H]^-$ are indicative of a carboxylic acid. For the fragment ion with *m/z* 544.2, cleavage between C_3 and C_4 in the aldohexonic acid is proposed, indicating that the aldohexonic acid is linked via C_4 to the adjacent hexose. Therefore, the structure Neu5Ac(α2–3) Gal(β1–4)GluconA is proposed, which represents the C_1-oxidized version of sialyllactose.

A glycan with the composition HS_2X (*m/z* 939.6) was observed at retention time 29.4 min (o8, Table 4-2). The MS/MS spectrum (Fig. 4-5C) shows the fragment ions B_1 (*m/z* 290.0), B_2 (*m/z* 581.3), Y_2 (*m/z* 357.1) and Y_3 (*m/z* 648.3), which is consistent with the sequence Neu5Ac–Neu5Ac–Hex–HexonA. The fragment ions Y_3-CO_2 (*m/z* 604.2) and $[M–CO_2–H]^-$ (*m/z* 895.4) are indicative of a carboxylic acid group.

A glycan with the composition H_2NX (*m/z* 722.4) was observed at retention time 21.4 min (o7, Table 4-2). The MS/MS spectrum (Fig. 4-5D) shows the fragment ions C_3 (*m/z* 543.9), Y_2 (*m/z* 357.0) and Y_3 (*m/z* 560.2), which is consistent with the sequence Hex–HexNAc–Hex–HexonA. For the fragment ions with masses *m/z* 586.2 and *m/z* 406.1, carbon chain cleavages at C_2–C_3 and C_4–C_5 of the aldohexonic acid are assumed. The fragment ion with mass m/z 406.1 originated from fragment ion Z_3. From these details, the structure Hex–HexNAc–Gal(β1–4)–HexonA (Fig. 4-2, o7) is proposed, which is interpreted as the C_1-oxidized version of oligosaccharide g7 (see above).

A glycan with the composition H_2NSX (*m/z* 1013.4) was detected at retention time 27.4 min (o9, Table 4-2).The fragment ions $[M–CO_2–H]^-$ (*m/z* 969.7) and $[M–CO_2–H_2O–H]^-$ (*m/z* 951.7) are indicative of a carboxylic acid group (Fig. 4-5E). For fragment ion $[M–CH_2OCH_2OCOO–H]^-$ (*m/z* 909.5), a cleavage between C_3 and C_4 of the aldohexonic acid is proposed. Moreover, the MS/MS spectrum shows the fragment ions $B_{2\alpha}$ (*m/z* 364.1), $Y_2Y_{2\beta}$ (*m/z* 357.1), $Z_{2\beta}$ (*m/z* 704.1), $Y_{2\beta}$ (*m/z* 722.3) and B_3 (*m/z* 817.5), which are consistent with the sequence Hex–HexNAc–[Neu5Ac]–Hex–HexonA.

Other C_1-oxidized oligosaccharide moieties were an aldohexonic acid carrying a sialic acid residue (o3), oligosaccharide o4, which represents a C_1-oxidized version of g3, and o5, which is interpreted as C_1-oxidized version of g5 (for details, see Table 4-2).

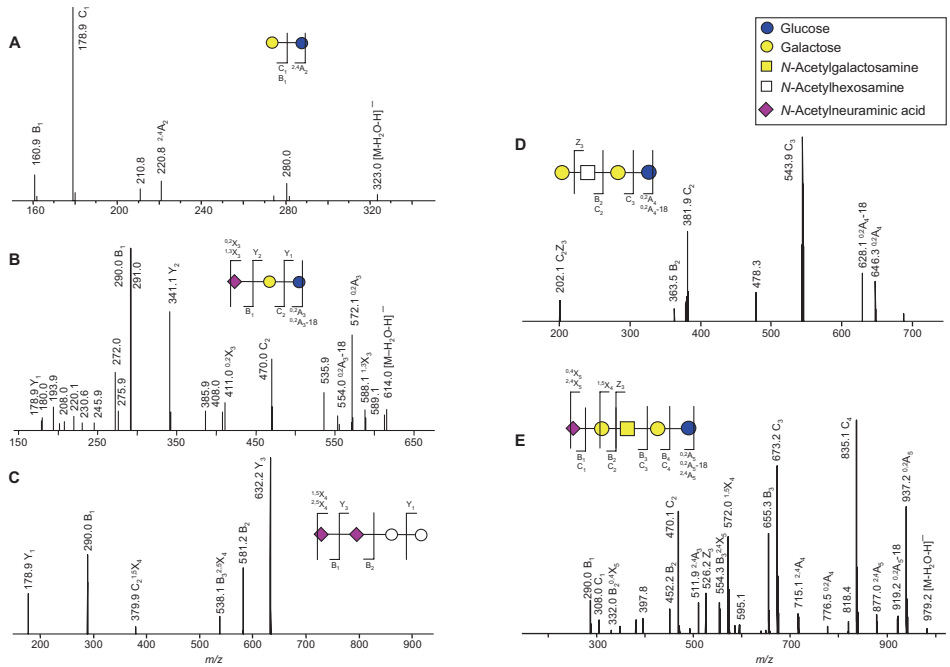

Figure 4-4. Negative-ion fragmentation mass spectra of oligosaccharides with reducing-end hexose residues with the proposed structures: (A) lactose, precursor ion *m/z* 341.2, g1; (B) sialyllactose, precursor ion *m/z* 632.2, g6; (C) lactose carrying a disialyl motif, precursor ion *m/z* 923.3, g9; (D) H_3N tetrasaccharide, precursor ion *m/z* 706.2, g7; (E) H_3NS pentasaccharide, precursor ion *m/z* 997.3, g10.

4.3.4 Glycan profiling of body fluids

LC-MS data were obtained for four urine samples from control individuals as well as seven urine samples, five amniotic fluid samples and two ascitic fluid samples from galactosialidosis patients. In the four urine samples of healthy controls, lactose (*m/z* 341.2), sialylhexose (*m/z* 470.2) and sialyllactose (*m/z* 632.2) were detected (data not shown). For the body fluid samples of galactosialidosis patients, the relative abundances of the mass spectrometric signals are given in Table 4-3. The two major classes of detected oligosaccharides are the endo-β-*N*-acetylglucosaminidase-cleaved products of complex-type sialylated *N*-glycans derivatives (n1–n6) and oligosaccharides with reducing-end hexose residues or disialyl motifs (g1–g11), with mean relative abundances of 37.1% and 44.8%, respectively. Sulfated glycans (s1–s4), which are presumably derived from complex-type *N*-glycans, accounted for a mean of 1.6% of all detected glycans. The relative abundance of aldohexonic acid-based oligosaccharides (o1–o9) differed considerably between urine samples on the one hand (mean 29.7%) and amniotic fluid and ascitic fluid samples on the other (mean 3.1%).

In all samples, the same set of complex-type *N*-glycan-derived structures was found, with the exception of H_5N_3S (n3) and $H_6N_4S_2$ (n5) in ascitic fluid samples Asf1 and Asf2, respectively (Table 4-3). In all samples, complex-type *N*-glycan derivatives with very high relative abundance were sialyl-*N*-acetyllactosamine (HNS; n1), disialylated diantennary structures

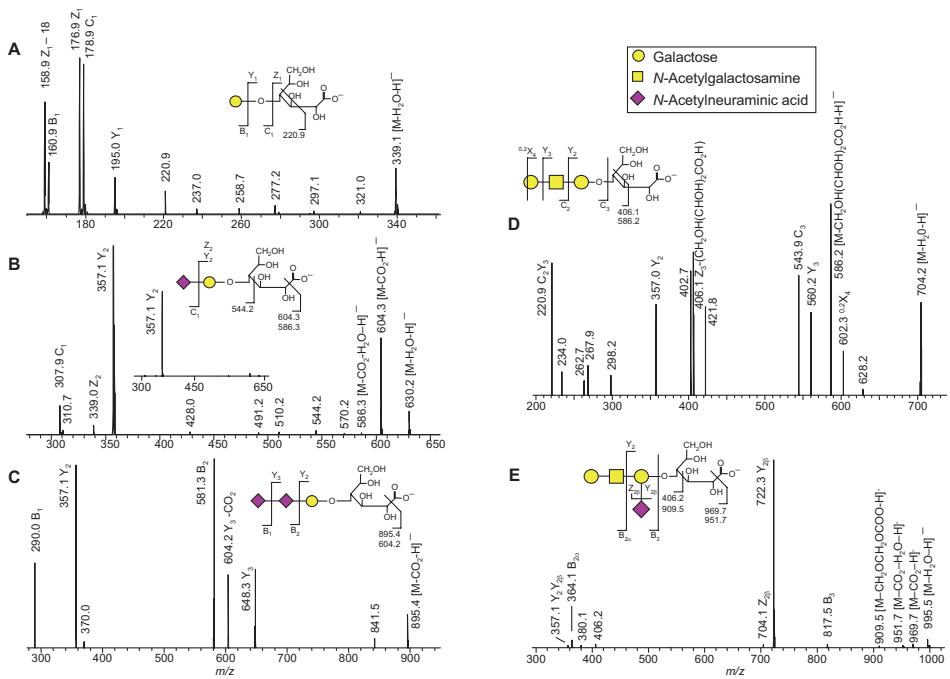

Figure 4-5. Negative-ion fragmentation mass spectra of C_1-oxidized oligosaccharides with the proposed structures: (A) C_1-oxidized lactose, precursor ion *m/z* 357.2, o2; (B) C_1-oxidized sialyllactose, precursor ion *m/z* 648.5, o6; (C) C_1-oxidized lactose carrying a disialyl motif, precursor ion *m/z* 939.6, o8; (D) C_1-oxidized version of H_3N tetrasaccharide, precursor ion *m/z* 722.4; o7; (E) C_1-oxidized version of the H_3NS pentasaccharide, precursor ion *m/z* 1013.4; o9.

($H_5N_3S_2$; n4) and sialylated monoantennary structures (H_3N_2S; n2). In amniotic fluid and ascitic fluid, tri-sialylated triantennary *N*-glycans ($H_6N_4S_3$; n6) were clearly next in order of relative abundance (Table 4-3).

Sulfated *N*-glycan derived structures were detected in all samples (Table 4-3). In three urine samples, the entire set of four sulfated *N*-glycans could be detected (Table 4-3, U2, U4 and U6). In one urine sample (U2), three isomers were detected for $H_5SO_3N_3S_2$ (data not shown).

Free oligosaccharides with reducing-end hexoses were detected in all samples. In two samples (Table 4-3, U1 and Amf5), the entire set of 11 oligosaccharides (g1–g11) was detected. The most abundant species of this glycan group in urine samples was sialyllactose (relative mean abundance 16.4% for g6, H_2S; Table 4-3), while the proposed sialylgalactose was the most abundant species in the amniotic and ascitic fluid samples (mean 20.4% for g2, HS; Table 4-3). Sialyllactose was observed with similar relative abundances in urine, amniotic and ascitic fluid samples (g6, Table 4-3). In urine sample U7, the relative amount of lactose was high (39.9%), and was one or two orders of magnitude lower for the other analyzed samples (g1, Table 4-3). The disialyl glycan (g4) was detected in all samples and had a mean relative abundance of 4.8%. Other glycans containing a disialyl motif (g9 and g11) were detected at low relative intensities (< 0.5%). Only in three of the 14 samples analyzed were neither of these species detected.

Table 4-3. Oligosaccharides observed in various body fluids of galactosialidosis patients. Mean retention time, mass to charge ratio and relative area are given for glycans detected in urine (U), amniotic fluid (Amf) or ascitic fluid (Asf). H, hexose; N, *N*-acetylhexosamine; S, *N*-acetylneuraminic acid; X, aldohexonic acid; SO_3, sulphate; +, trace amount; –, not detected.

				Sample:		U1	U2	U3	U4
	Fig. 2	**Composition**	***m/z***	**charge**	**Ret. Time**	**%**	**%**	**%**	**%**
With reducing-end	n1	HNS	673,4	$[M^-H]^-$	22.3	4,1	14,5	18,3	15,9
	n2	H_3N_2S	1200,4	$[M^-H]^-$	23.0	2,8	10,6	3,4	7,5
	n3	H_5N_3S	1727,8	$[M^-H]^-$	23.9	0,3	0,6	0,2	0,6
	n4	$H_5N_3S_2$	1009,0	$[M^-2H]^{2-}$	27.3	5,9	17,6	3,6	9,6
	n5	$H_6N_4S_2$	1191,4	$[M^-2H]^{2-}$	27.4	0,5	1,3	0,5	1,1
	n6	$H_6N_4S_3$	891,3	$[M^-3H]^{3-}$	31.3	0,4	1,2	0,5	1,2
						14,1	45,7	26,5	36,0
Sulfated glycans	s1	H(S)NS	753,2	$[M^-H]^-$	32.0	0,3	0,6	1,4	2,3
	s2	$H_3(S)N_2S$	639,7	$[M^-2H]^{2-}$	36.5	0,3	1,3	-	0,5
	s3	$H_5(S)N_3S$	903,3	$[M^-2H]^{2-}$	34.6	-	0,3	-	0,2
	s4	$H_5(S)N_3S_2$	1048,8	$[M^-2H]^{2-}$	39.6	+	0,2	0,1	0,2
						0,6	2,4	1,5	3,2
With reducing-end hexose or disyalyl motif	l1	H_2	341,2	$[M^-H]^-$	7.6	1,2	1,9	5,3	3,6
	l2	HS	470,2	$[M^-H]^-$	24.4	3,4	4,4	9,4	8,6
	l3	H_3	503,2	$[M^-H]^-$	9.1	0,2	3,4	3,5	3,2
	l4	S_2	599,2	$[M^-H]^-$	27.7	3,3	4,2	4,9	8,2
	l5	H_2N	544,2	$[M^-H]^-$	9.6	0,9	1,8	3,4	4,3
	l6	H_2S	632,2	$[M^-H]^-$	22.7	8,1	10,8	29,9	22,2
	l7	H_3N	706,2	$[M^-H]^-$	12.7	1,8	0,8	2,4	0,8
	l8	H_2NS	835,3	$[M^-H]^-$	22.8	1,5	4,1	2,0	4,2
	l9	H_2S_2	923,3	$[M^-H]^-$	29.1	+	0,1	-	-
	l10	H_3NS	997,3	$[M^-H]^-$	22.0	0,7	0,4	0,2	0,5
	l11	H_3NS_2	643,7	$[M^-2H]^{2-}$	29.5	0,4	-	0,1	0,1
						21,6	31,8	61,0	55,7
With terminal aldohexonic acid	o1	X	195,1	$[M^-H]^-$	13.3	62,3	1,6	1,0	2,0
	o2	HX	357,2	$[M^-H]^-$	19.2	0,8	17,3	3,0	2,2
	o3	SX	486,1	$[M^-H]^-$	26.4	0,2	0,1	-	0,2
	o4	H_2X	519,2	$[M^-H]^-$	22.6	0,3	0,9	-	-
	o5	HNX	560,2	$[M^-H]^-$	24.3	0,2	0,1	6,1	0,3
	o6	HSX	648,5	$[M^-H]^-$	26.0	-	-	0,8	0,5
	o7	H_2NX	722,4	$[M^-H]^-$	21.4	-	-	-	-
	o8	HS_2X	939,6	$[M^-H]^-$	29.4	-	+	0,1	-
	o9	H_2NSX	1013,4	$[M^-H]^-$	27.4	-	-	-	-
						63,7	20,1	11,1	5,2

U5 %	U6 %	U7 %	Avg U %	Amf1 %	Amf2 %	Amf3 %	Amf4 %	Amf5 %	Asf1 %	Asf2 %	Avg A %	Avg OA %
15,1	9,6	15,0	13,2	22,5	19,9	22,7	25,4	20,5	19,2	19,1	21,3	17,3
0,9	4,0	0,5	4,2	6,0	7,3	5,0	4,7	4,7	3,7	5,8	5,3	4,8
0,2	0,4	0,1	0,3	+	0,5	0,2	0,8	0,3	-	0,1	0,4	0,4
2,2	5,5	1,2	6,5	18,7	22,3	16,5	17,5	22,0	9,1	14,3	17,2	11,9
0,4	0,4	0,1	0,6	1,2	1,4	0,9	1,4	1,5	0,4	-	1,1	0,8
0,3	0,2	0,2	0,6	5,2	4,8	3,5	3,4	4,9	1,3	2,6	3,7	2,1
19,2	20,0	17,0	25,5	53,6	56,2	48,9	53,2	53,9	33,8	41,8	48,8	37,1
2,3	0,6	0,3	1,1	-	-	-	0,4	0,7	0,7	3,0	1,2	1,1
+	0,3	-	0,6	0,8	1,3	0,9	0,9	1,0	-	-	1,0	0,8
+	0,2	-	0,2	0,3	-	0,4	-	-	0,4	-	0,4	0,3
-	+	-	0,1	-	-	-	-	0,6	-	-	0,6	0,3
2,4	1,1	0,3	1,6	1,1	1,3	1,4	1,3	2,2	1,1	3,0	1,6	1,6
4,2	1,2	39,9	8,2	0,9	0,4	-	0,7	1,5	2,3	2,3	1,3	5,0
6,0	2,6	5,1	5,6	19,1	14,4	21,9	14,7	13,4	36,1	23,1	20,4	13,0
3,1	-	2,9	2,7	-	-	-	-	0,6	-	-	0,6	2,4
7,2	4,3	0,9	4,7	3,0	5,0	5,6	7,3	6,8	2,4	4,6	5,0	4,8
3,3	0,9	1,6	2,3	1,2	0,8	0,9	1,3	1,1	0,9	1,1	1,1	1,7
17,2	6,5	20,2	16,4	12,3	14,3	14,7	16,4	14,2	17,8	17,8	15,4	15,9
0,4	0,5	0,3	1,0	0,2	-	-	0,4	0,1	-	-	0,2	0,8
0,9	1,9	0,6	2,2	4,1	3,5	4,0	2,1	3,4	1,0	3,5	3,1	2,6
0,1	+	+	0,1	-	0,3	-	0,2	0,4	-	0,3	0,3	0,2
0,1	0,2	+	0,3	0,3	-	-	0,3	0,3	-	-	0,3	0,3
-	-	-	0,2	-	-	-	-	0,2	-	-	0,2	0,2
42,3	18,1	71,6	43,1	41,1	38,6	47,1	43,6	41,9	60,6	52,8	46,5	44,8
3,1	18,6	8,9	13,9	0,9	-	-	-	1,1	2,2	+	1,4	10,2
27,9	37,0	1,5	12,8	1,3	1,0	-	1,3	0,2	0,9	1,8	1,1	7,4
0,2	0,1	-	0,2	0,4	0,5	-	-	0,4	-	-	0,4	0,3
1,5	0,5	-	0,8	1,5	1,6	2,3	-	-	1,5	-	1,7	1,3
0,9	0,2	0,5	1,2	0,1	0,7	0,4	0,6	0,3	-	0,6	0,4	0,8
2,7	3,8	-	1,9	-	-	-	-	-	-	-		1,9
-	0,2	-	0,2	-	-	-	-	-	-	-		0,2
-	0,2	0,1	0,1	-	-	-	-	-	-	-		0,1
-	0,3	+	0,3	-	-	-	-	-	-	-		0,3
36,1	60,8	11,1	29,7	4,2	3,9	2,7	1,9	2,0	4,6	2,4	3,1	16,4

In the amniotic and ascitic fluid samples, aldohexonic acid-containing oligosaccharides o1–o5 were detected. In the urine samples, high levels of aldohexonic acid-containing glycans were often observed, with the exception of U4 (Table 4-3). In U1, U6 and U7, gluconic acid (o1) has high abundance, and high levels of C_1-oxidized lactose (o2) were observed in urine samples U2, U5 and U6.

4.4 DISCUSSION

Using a prototype capillary HPAEC-PAD-MS system, we observed *N*-glycan-derived oligosaccharide structures (Fig. 4-2, n1–6) in urine, amniotic fluid and ascitic fluid samples from various galactosialidosis patients as described previously [12]. The new set-up also allowed detection of new oligosaccharides in the samples from galactosialidosis patients: (a) *O*-sulfated oligosaccharide moieties, (b) carbohydrate moieties with reducing-end hexoses, and (c) oligosaccharides with C_1-oxidized hexose. The detection of relatively low amounts of *O*-sulfated oligosaccharide moieties and C_1-oxidized carbohydrate moieties, especially in the amniotic and ascitic fluid samples, is made possible by the sensitivity gain achieved by coupling of a capillary HPAEC-PAD to the MS system compared to use of a normal-bore HPAEC-PAD [13,19]. Importantly, the analytical setup allows analysis of glycans with reducing ends, reduced termini and C_1 oxidation, which makes it more broadly applicable than methods that depend on reducing ends for reductive amination reactions [20]. An important aspect of HPAEC is its ability to separate structural isomers, as documented previously [13,15]. Hence, HPAEC-PAD-MS represents a valuable addition to the repertoire of LC-MS methods for oligosaccharide analysis.

Almost all carbohydrate structures described here are terminated with galactose and / or sialic acid residues, which can be explained by the defect of cathepsin A in galactosialidosis patients, resulting in insufficient protection of β-galactosidase and α-neuraminidase against excessive intra-lysosomal degradation [2]. Cathepsin A is one of four enzymes in a lysosomal multi-enzyme complex comprising *N*-acetylgalactosamine-6-sulfate sulfatase, β-galactosidase, cathepsin A and α-neuraminidase [3,4].

The enzyme *N*-acetylgalactosamine-6-sulfatase or galactose-6-sulfatase has been shown to be specific for 6-sulfated galactose and *N*-acetylgalactosamine [21,22]. The structures s1–s4 (Fig. 4-2) are interpreted as being derived from complex-type *N*-linked carbohydrates. 6'-sulfated sialyllactosamine (s1) has also been found on *O*-linked glycan moieties [18], which may therefore represent an alternative source of this glycan.

Tandem mass spectrometry provided evidence that at least some of the oligosaccharide chains with hexose at the reducing end have a Gal(β1–4)Glc (lactose) core structure. This group of glycans (g1–g11) shares structural features with milk oligosaccharides, plasma oligosaccharides and previously described urinary oligosaccharides from healthy individuals [23-25]. The structures g1 and g6 in Fig. 4-2 can be interpreted as lactose (g1) and sialyllactose (g6), which are known to be present in various body fluids [24,26-28]. Moreover, the tetrasaccharide g7 may be interpreted as lacto-*N*-tetraose, and g10 may represent a sialylated version thereof. As these structures are in part identical with milk sugars, they may be of limited diagnostic value. Several glycosyltransferases have been identified in urine and amniotic fluid [29-32], but no-one, to the best of our knowledge, has demonstrated that glycosyltransferases are active in these fluids.

Notably, the detected structures g4 (S_2), g8 (H_2NS), g9 (H_2S_2), g10 (H_3NS) and g11 (H_3NS_2) all exhibited structural motifs that are typically found on glycosphingolipids. g4 is interpreted as a predominantly glycosphingolipid-derived disialyl motif, and the oligosaccharides g8, g9, g10 and g11 are postulated to represent, at least in part, reducing-end glycan moieties of the gangliosides GM2, GD3, GM1 and GD1b, respectively (Fig. 4-2, g8–g11). In addition, the structures g5 and g7 may also be interpreted as partly glycosphingolipids derived (ganglio-, lacto- or lactoneo- series).

To our knowledge, such intact oligosaccharide moieties have hitherto not been described as glycosphingolipids degradation products. According to the literature, catabolism of glycosphingolipids starts from the non-reducing end while the glycan is still bound to the ceramide, and is performed by a variety of exoglycosidases, which are often also involved in the degradation of *N*-glycans and *O*-glycans [33,34]. This process leads to the release of monosaccharides and results in glucosylceramide and galactosylceramide, which may be degraded further by glycosidic bond cleavage. Additional proteins such as saposins (sphingolipid activator proteins) are required for the catabolism of glycosphingolipids [35]. A blockage of glycosphingolipid degradation, as occurs in Fabry's disease as a result of a lack of α-galactosidase activity, leads to accumulation of the glycosphingolipid substrate, which in Fabry's disease is globotriaosylceramide [34]. Consequently, in galactosialidosis, only intact glycosphingolipids would be expected to be secreted, not the glycan moieties as described here. Our finding of free oligosaccharide moieties presumably derived from glycosphingolipids implies the existence of an endoglycosylceramidase involved in an alternative glycosphingolipid catabolic pathway. While such an enzyme has not been described for vertebrates, endoglycoceramidases (EC 3.2.1.123) have been found and characterized for invertebrates [36-39]. The enzymatic activity of the postulated endoglycoceramidase may depend on saposins [35], and may represent a side activity of glucosylceramidase (EC 3.2.1.45) facilitated by specific saposins. With regard to the disaccharide of two sialic acid residues (Fig. 4-2, g4), it is unclear which enzyme would catalyze the release of this disaccharide unit from gangliosides.

The last group of newly found oligosaccharides is characterized by C_1-oxidized hexose residues (o1–o9). This group of glycans appears to be strongly related to the above-described glycans with reducing-end hexoses (g1–g11), suggesting C_1 oxidation of these oligosaccharide moieties. The glycans o8 and o9 may be interpreted as C_1-oxidized versions of ganglioside-derived glycan moieties (Fig. 4-2). The C_1-oxidized oligosaccharides were found in urine samples at relatively high amounts (mean 30%; Table 4-3). C_1-oxidized carbohydrate moieties were also found in amniotic fluid samples, albeit at lower relative amounts (mean 3%; Table 4-3). The cause of C_1 oxidation of the reducing end is unknown. We can exclude the possibility that these species were observed due to oxidation of reducing sugars during the chromatographic process and the subsequent MS detection, as we observed chromatographic separation of the reducing glycans from the C_1-oxidized species, clearly indicating that these species were already present in the samples prior to HPAECPAD-MS analysis. With regard to the origin of the C_1-oxidized glycans, it is possible to speculate about a non-enzymatic oxidation reaction that may have occurred before the urine and amniotic samples were collected, or during sample storage. Alternatively, an enzymatic oxidation may be postulated. The possibility that an enzyme of microbial origin is responsible, as described for *Escherichia coli* [40-44], appears not to be likely, as the oxidation products were not only observed in urine samples, but also in amniotic fluid, which is considered

to be sterile. Alternatively, it could be speculated that a human enzymatic activity might be present in the liver or kidney, for example, that causes C_1 oxidation of glycosphingolipid glycan moieties. This enzyme may act in conjunction with the postulated endoglycoceramidase.

Together with our previous study on G_{M1} gangliosidosis [13], this study shows the potential value of capillary HPAEC-PAD-MS for analyzing oligosaccharides from clinical samples. This prototype analytical system features femtomolar sensitivity for both pulsed amperometric detection and mass spectrometric detection [13]. Moreover, it allows the analysis of oligosaccharides in both positive-ion mode [13] and negative-ion mode, as shown here. Based on the excellent MS/MS features of the ion trap mass spectrometer, informative fragment spectra of sodium adducts [13] and deprotonated species (this study) can be obtained with minute amounts of material, thus allowing insights into defects of glycoconjugate degradation and lysosomal storage diseases.

4.5 EXPERIMENTAL PROCEDURES

4.5.1 Materials

Analytical reagent-grade sodium hydroxide (50% w/w), sodium acetate, sulfuric acid and sodium chloride were obtained from J.T. Baker (Deventer, The Netherlands). Acetonitrile was obtained from Biosolve (Valkenswaard, The Netherlands). All solutions were prepared using water from a Milli-Q synthesis system from Millipore BV (Amsterdam, The Netherlands). Details of the urine, amniotic fluid and ascitic fluid samples are given in Table 4-1.

4.5.2 Capillary HPAEC

The capillary chromatographic system consists of a modified BioLC system from Dionex (Sunnyvale, CA), comprising a microbore GP40 gradient pump, a Famos micro autosampler with a full polyaryletherketone (PAEK) injector equipped with a 1 µL loop, and an ED40 electrochemical detector. BioLC control, data acquisition from the ED40 detector and signal integration are supported by chromeleon software (Dionex). This modified system has been described in detail previously [13]. A prototype capillary column 250 mm long with internal diameter 0.4 mm, packed with CarboPac PA200 resin, was manufactured by Dionex. The GP40 flow rate was 0.53 mL•min^{-1}, and the eluent flow was split using a custom-made polyether ether ketone (PEEK) splitter to 10 µL·min^{-1}. The pump was provided with the following eluents: eluent A, water; eluent B, 500 mM NaOH; eluent C, 500 mM NaOAc. All separations were performed at room temperature. The following ternary gradient was used for the separation: 76% A + 24% B (–20 to –14 min), isocratic sodium hydroxide wash; 88% A + 12% B (–14 to 0 min), isocratic equilibration of the column; 42.6% A + 12% B + 45.4% C (0–40 min), linear sodium acetate gradient was used for the separation. The ED40 detector applies the following waveform to the electrochemical cell: E_1 = 0.1 V (t_d = 0.00–0.20 s, t_1 = 0.20–0.40 s), E_2 = –2.0 V (t_2 = 0.41–0.42 s), E_3 = 0.6 V (t_3 = 0.43 s), E_4 = –0.1 V (t_4 = 0.44–0.50 s) versus an Ag/AgCl reference electrode [45]. A gold work electrode and a 25 µm gasket were installed.

4.5.3 Mass spectrometry

Coupled to the chromatographic system was an Esquire 3000 ion-trap mass spectrometer from Bruker Daltonics (Bremen, Germany), equipped with an electrospray ionization source.

To convert the HPAEC eluate into an ESI-compatible solution, an in-line prototype desalter (Dionex) was used, continuously regenerated with diluted sulfuric acid [13]. A modified microbore AGP-1 from Dionex was used as an auxiliary pump: to obtain efficient ionization of the eluted carbohydrates, 50% acetonitrile was pumped into the eluent flow via a MicroTEE (P-775, Upchurch Scientific, Oak Harbor, WA, USA) at a flow rate of 4.6 µl·min^{-1}. The mixture was directed to the electrospray ionization interface of the Esquire 3000. The carbohydrates were detected using the MS in the negative-ion mode. The MS was operated under the following conditions: dry temperature 325 °C, nebulizer 103 kPa, dry gas 7 L·min^{-1}, target mass *m/z* 850, scan speed 13 000 *m/z* per s in MS and MS/MS mode. For tandem MS, automatic selection of three precursors was applied.

4.5.4 Sample preparation

Oligosaccharides of the samples were isolated by graphitized carbon solid-phase extraction, as described previously [46]. A 200 µL sample was diluted with 1800 µL demineralized water and loaded on a Carbograph SPE (210142) from Alltech Associates Inc. (Deerfield, IL, USA). The cartridge was washed with 6 mL of demineralized water. The oligosaccharides were eluted from the column using 3 mL of 25% acetonitrile containing 0.05% trifluoroacetic acid. The eluate was evaporated under a nitrogen stream at room temperature until the volume had decreased by 50%. The remaining solution was lyophilized and reconstituted with 200 µL demineralized water.

4.6 ACKNOWLEDGEMENTS

We would like to thank Professor Ron Wevers (Radboud University Nijmegen Medical Center, The Netherlands) and Dr Pim Onkenhout (Leiden University Medical Center, The Netherlands) for kindly providing samples, Dr Cornelis H. Hokke for fruitful discussions, Rob Bruggink for providing essential input for producing the capillary desalter, and Chris Pohl, Yan Liu, Victor Barretto and Franck van Veen from Dionex for essential support of this research.

REFERENCES

1. Wenger DA, Tarby TJ, & Wharton C (1978) Macular cherry-red spots and myoclonus with dementia: coexistent neuraminidase and beta-galactosidase deficiencies. *Biochem Biophys Res Commun* **82,** 589-595.
2. D'Azzo A, Hoogeveen A, Reuser AJ, Robinson D, & Galjaard H (1982) Molecular defect in combined beta-galactosidase and neuraminidase deficiency in man. *Proc Natl Acad Sci U S A* **79,** 4535-4539.
3. Pshezhetsky AV & Potier M (1996) Association of N-acetylgalactosamine-6-sulfate sulfatase with the multienzyme lysosomal complex of beta-galactosidase, cathepsin A, and neuraminidase. Possible implication for intralysosomal catabolism of keratan sulfate. *J Biol Chem* **271,** 28359-28365.
4. Pshezhetsky AV & Ashmarina M (2001) Lysosomal multienzyme complex: biochemistry, genetics, and molecular pathophysiology. *Prog Nucleic Acid Res Mol Biol* **69,** 81-114.
5. Lowden JA & O'Brien JS (1979) Sialidosis: a review of human neuraminidase deficiency. *Am J Hum Genet* **31,** 1-18.
6. Takahashi Y, Nakamura Y, Yamaguchi S, & Orii T (1991) Urinary oligosaccharide excretion and severity of galactosialidosis and sialidosis. *Clin Chim Acta* **203,** 199-210.
7. Groener J, Maaswinkel-Mooy P, Smit V, van der Hoeven M, Bakker J, Campos Y, & D'Azzo A (2003) New mutations in two Dutch patients with early infantile galactosialidosis. *Mol Genet Metab* **78,** 222-228.

8. Okamura-Oho Y, Zhang S, & Callahan JW (1994) The biochemistry and clinical features of galactosialidosis. *Biochim Biophys Acta* **1225,** 244-254.
9. Sewell AC (1981) Simple laboratory determination of excess oligosaccharidurie. *Clin Chem* **27,** 243-245.
10. van Pelt J, Kamerling JP, Vliegenthart JF, Hoogeveen AT, & Galjaard H (1988) A comparative study of the accumulated sialic acid-containing oligosaccharides from cultured human galactosialidosis and sialidosis fibroblasts. *Clin Chim Acta* **174,** 325-335.
11. van Pelt J, Kamerling JP, Vliegenthart JF, Verheijen FW, & Galjaard H (1988) Isolation and structural characterization of sialic acid-containing storage material from mucolipidosis I (sialidosis) fibroblasts. *Biochim Biophys Acta* **965,** 36-45.
12. van Pelt J, Hard K, Kamerling JP, Vliegenthart JF, Reuser AJ, & Galjaard H (1989) Isolation and structural characterization of twenty-one sialyloligosaccharides from galactosialidosis urine. An intact N,N'-diacetylchitobiose unit at the reducing end of a diantennary structure. *Biol Chem Hoppe Seyler* **370,** 191-203.
13. Bruggink C, Wuhrer M, Koeleman CA, Barreto V, Liu Y, Pohl C, Ingendoh A, Hokke CH, & Deelder AM (2005) Oligosaccharide analysis by capillary-scale high-pH anion-exchange chromatography with on-line ion-trap mass spectrometry. *J Chromatogr B Analyt Technol Biomed Life Sci* **829,** 136-143.
14. Ramsay SL, Maire I, Bindloss C, Fuller M, Whitfield PD, Piraud M, Hopwood JJ, & Meikle PJ (2004) Determination of oligosaccharides and glycolipids in amniotic fluid by electrospray ionisation tandem mass spectrometry: in utero indicators of lysosomal storage diseases. *Mol Genet Metab* **83,** 231-238.
15. Townsend RR, Hardy MR, Hindsgaul O, & Lee YC (1988) High-performance anion-exchange chromatography of oligosaccharides using pellicular resins and pulsed amperometric detection. *Anal Biochem* **174,** 459-470.
16. Harvey DJ (2005) Fragmentation of negative ions from carbohydrates: part 3. Fragmentation of hybrid and complex N-linked glycans. *J Am Soc Mass Spectrom* **16,** 647-659.
17. Pfenninger A, Karas M, Finke B, & Stahl B (2002) Structural analysis of underivatized neutral human milk oligosaccharides in the negative ion mode by nano-electrospray MS^n (part 1: methodology). *J Am Soc Mass Spectrom* **13,** 1331-1340.
18. Hemmerich S, Leffler H, & Rosen SD (1995) Structure of the O-glycans in GlyCAM-1, an endothelial-derived ligand for L-selectin. *J Biol Chem* **270,** 12035-12047.
19. van der Hoeven RAM, Hofte AJP, Tjaden UR, van der Greef J, Torto N, Gorton L, Marko-Varga G, & Bruggink C (1998) Sensitivity improvement in the analysis of oligosaccharides by online high-performance anion-exchange chromatography/ionspray mass spectrometry. *Rapid Commun Mass Spectrom* **12,** 69-74.
20. Anumula KR (2006) Advances in fluorescence derivatization methods for high-performance liquid chromatographic analysis of glycoprotein carbohydrates. *Anal Biochem* **350,** 1-23.
21. Glossl J, Truppe W, & Kresse H (1979) Purification and properties of N-acetylgalactosamine 6-sulphate sulphatase from human placenta. *Biochem J* **181,** 37-46.
22. Glossl J & Kresse H (1982) Impaired degradation of keratan sulphate by Morquio A fibroblasts. *Biochem J* **203,** 335-338.
23. Koseki M & Tsurumi K (1977) A convenient method for the isolation of 3'-sialyllactose from normal human urine. *J Biochem* **82,** 1785-1788.
24. Arthur PG, Kent JC, & Hartmann PE (1989) Microanalysis of the metabolic intermediates of lactose synthesis in human milk and plasma using bioluminescent methods. *Anal Biochem* **176,** 449-456.
25. Ninonuevo MR, Park Y, Yin H, Zhang J, Ward RE, Clowers BH, German JB, Freeman SL, Killeen K, Grimm R, & Lebrilla CB (2006) A strategy for annotating the human milk glycome. *J Agric Food Chem* **54,** 7471-7480.
26. Ramsay SL, Meikle PJ, Hopwood JJ, & Clements PR (2005) Profiling oligosaccharidurias by electrospray tandem mass spectrometry: quantifying reducing oligosaccharides. *Anal Biochem* **345,** 30-46.
27. An Y, Young SP, Hillman SL, Van Hove JL, Chen YT, & Millington DS (2000) Liquid chromatographic assay for a glucose tetrasaccharide, a putative biomarker for the diagnosis of Pompe disease. *Anal Biochem* **287,** 136-143.
28. Maury CP & Wegelius O (1981) Urinary sialyloligosaccharide excretion as an indicator of disease activity in rheumatoid arthritis. *Rheumatol Int* **1,** 7-10.
29. Chester MA (1974) The occurrence of a beta-galactosyltransferase in normal human urine. *FEBS Lett* **46,** 59-62.
30. Serafini-Cessi F, Malagolini N, & Dall'Olio F (1988) Characterization and partial purification of beta-N-acetylgalactosaminyltransferase from urine of Sd(a+) individuals. *Arch Biochem Biophys* **266,** 573-582.
31. Nelson JD, Jato-Rodriguez JJ, & Mookerjea S (1973) Occurrence of soluble glycosyltransferases in human amniotic fluid. *Biochem Biophys Res Commun* **55,** 530-537.

32. Nelson JD, Jato-Rodriguez JJ, & Mookerjea S (1974) The occurrence and properties of soluble UDP-galactose:glycoprotein galactosyltransferase in human amniotic fluid. *Can J Biochem* **52,** 42-50.
33. Sandhoff K & Kolter T (2003) Biosynthesis and degradation of mammalian glycosphingolipids. *Philos Trans R Soc Lond B Biol Sci* **358,** 847-861.
34. Kolter T & Sandhoff K (2006) Sphingolipid metabolism diseases. *Biochim Biophys Acta* **1758,** 2057-2079.
35. Kolter T & Sandhoff K (2005) Principles of lysosomal membrane digestion: stimulation of sphingolipid degradation by sphingolipid activator proteins and anionic lysosomal lipids. *Annu Rev Cell Dev Biol* **21,** 81-103.
36. Ito M & Yamagata T (1986) A novel glycosphingolipid-degrading enzyme cleaves the linkage between the oligosaccharide and ceramide of neutral and acidic glycosphingolipids. *J Biol Chem* **261,** 14278-14282.
37. Ito M & Yamagata T (1989) Purification and characterization of glycosphingolipid-specific endoglycosidases (endoglycoceramidases) from a mutant strain of Rhodococcus sp. Evidence for three molecular species of endoglycoceramidase with different specificities. *J Biol Chem* **264,** 9510-9519.
38. Li YT & Li SC (1989) Ceramide glycanase from leech, Hirudo medicinalis, and earthworm, Lumbricus terrestris. *Methods Enzymol* **179,** 479-487.
39. Horibata Y, Sakaguchi K, Okino N, Iida H, Inagaki M, Fujisawa T, Hama Y, & Ito M (2004) Unique catabolic pathway of glycosphingolipids in a hydrozoan, Hydra magnipapillata, involving endoglycoceramidase. *J Biol Chem* **279,** 33379-33389.
40. Hugh R & Leifson E (1953) The taxonomic significance of fermentative versus oxidative metabolism of carbohydrates by various gram negative bacteria. *J Bacteriol* **66,** 24-26.
41. Taylor WH & Juni E (1961) Pathways for biosynthesis of a bacterial capsular polysaccharide. I. Carbohydrate metabolism and terminal oxidation mechanisms of a capsuleproducing coccus. *J Bacteriol* **81,** 694-703.
42. Hommes RW, Postma PW, Tempest DW, Neijssel OM, Dokter P, & Dione JA (1984) Evidence of a quinoprotein glucose dehydrogenase apoenzyme in several strains of *Escherichia coli*. *FEMS Microbiol Lett* **24,** 329-333.
43. Liu ST, Lee LY, Tai CY, Hung CH, Chang YS, Wolfram JH, Rogers R, & Goldstein AH (1992) Cloning of an *Erwinia herbicola* gene necessary for gluconic acid production and enhanced mineral phosphate solubilization in *Escherichia coli* HB101: nucleotide sequence and probable involvement in biosynthesis of the coenzyme pyrroloquinoline quinone. *J Bacteriol* **174,** 5814-5819.
44. Yan Z, Caldwell GW, & McDonell PA (1999) Identification of a gluconic acid derivative attached to the N-terminus of histidine-tagged proteins expressed in bacteria. *Biochem Biophys Res Commun* **262,** 793-800.
45. Rocklin RD, Clarke AP, & Weitzhandler M (1998) Improved long-term reproducibility for pulsed amperometric detection of carbohydrates via a new quadruple-potential waveform. *Anal Chem* **70,** 1496-1501.
46. Packer NH, Lawson MA, Jardine DR, & Redmond JW (1998) A general approach to desalting oligosaccharides released from glycoproteins. *Glycoconj J* **15,** 737-747.